



## Partitioning of star branched polymers into pores at three chromatography conditions

Yongmei Wang\*, Aaron Masur, Yutian Zhu, Jesse Ziebarth

Department of Chemistry, The University of Memphis, Memphis, TN 38152, USA

### ARTICLE INFO

#### Article history:

Received 11 May 2010

Received in revised form 20 July 2010

Accepted 27 July 2010

Available online 3 August 2010

#### Keywords:

Star-shaped polymers

Polymer partitioning

Monte Carlo simulation

Excluded volume effect

Liquid chromatography at the critical condition

### ABSTRACT

The partitioning of star branched polymers into a slit pore at three different chromatography conditions, namely, size exclusion chromatography (SEC), liquid chromatography at the critical condition (LCCC), and liquid adsorption chromatography (LAC) have been investigated with lattice Monte Carlo simulations. Two different chain models are used: random walks (RW) that have no excluded volume interaction and self-avoiding walks (SAW) that have excluded volume interaction. The simulation data obtained for the two chain models are compared to illustrate the effect of excluded volume interactions on the partitioning of star branched polymers. The two most outstanding effects observed due to the introduction of excluded volume interactions are: (i) stars with a high number of arms can be excluded from the pore at condition corresponding to the LCCC of the linear polymers; (ii) the partition coefficient of stars in LAC mode is not dependent only on the total number of monomers on the chain. These effects illustrated by the current study should be taken into account when interpreting experimental chromatography data for branched polymers.

© 2010 Elsevier B.V. All rights reserved.

### 1. Introduction

The simplest and first-implemented chromatographic technique for polymer separation is size exclusion chromatography (SEC), also known as gel permeation chromatography (GPC). In SEC, polymers are typically dissolved in a thermodynamic good solvent to minimize any potential adsorption on column substrate and solutions are passed through a column filled with porous media. High molecular weight polymers with large size are excluded from the pores and are eluted first, while low molecular weight polymers with smaller size are able to fit into pores in the column, become temporarily trapped or diverted from the main paths and thus elute later. Hence separation of polymers according to size, or more precisely the hydrodynamic volume, is achieved in SEC [1]. Successful applications of SEC require that the polymers do not interact with the column substrate other than by steric exclusion from the porous surface.

The desire to separate polymers according to properties other than their sizes has led to the development of other chromatographic methods such as liquid adsorption chromatography (LAC), gradient liquid adsorption chromatography, precipitation–redissolution chromatography and liquid chromatography at the critical condition (LCCC), etc. [2,3]. These chromatography methods generally operate in a mode where poly-

mer interaction with the column substrate is no longer just steric exclusion, but also includes polymers adsorption and desorption from the porous substrate during the separation process. LCCC in particular has attracted a great deal of attention both because of its value in practical applications and the intricate theoretical basis for the existence of such condition. The so-called critical condition refers to the chromatography condition point at which the elution time of homopolymers becomes independent of their molecular weights. This chromatography condition in most cases corresponds to the critical adsorption point (CAP) of polymers on porous substrate [4–9] hence it is a thermodynamically well-defined point. However, there are other ways to achieve separation with this critical condition like behavior, which does not correspond to the CAP, such as in limiting chromatography proposed by Berek in a few recent papers [10,11].

Theoretical understanding of how polymers elute in chromatography separations is always important to actual experimental applications. The theory that best explain polymer separations in liquid chromatography was initially formulated by Casassa for SEC [12,13] and later extended by several Russian investigators for LCCC and LAC [5,8,14,15]. The value of these theoretical investigations should not be underestimated, as evidenced by a number of joint papers of these investigators with different experimental groups [2,8,16]. The theoretical calculation amounts to the determination of the partition coefficient  $K$  of a polymer chain when placed in a pore environment vs. a polymer chain placed in a free bulk solution. By adopting a Gaussian chain model for polymers, one can easily calculate  $K$  for a variety of different situations (i.e., linear chains,

\* Corresponding author. Tel.: +1 901 678 2629; fax: +1 901 678 3447.  
E-mail address: [ywang@memphis.edu](mailto:ywang@memphis.edu) (Y. Wang).

ring, stars, block copolymers with two chemically different blocks, etc.). However, those theoretical calculations have treated the polymer chains with the Gaussian chain model. In the Gaussian chain model, the excluded volume interaction between monomers along the chain is not taken into account. The effect of excluded volume interaction on polymer conformational properties has long been known to be important and the effect is exemplified when chains are confined in pores. Scaling theory has been particularly helpful in illustrating the effect of excluded volume interaction on chain conformational properties [17]. For example, de Gennes pointed out that when a chain is placed inside the pore, the longitudinal dimension of the chain along the pore will not be perturbed if one treats the chain by the Gaussian chain model, however, the chain should be stretched in the longitudinal dimension if one considers the excluded volume interaction [17]. On the other hand, the partition coefficient  $K$  can also be determined by computer simulations using either lattice or off-lattice models for polymer chains. One advantage of computer simulation over analytical theory is that in computer simulation one can choose different chain models, either using random walks (RW), which are nearly equivalent to the Gaussian chain model, or self-avoiding walks which have the excluded volume interaction. Hence, by comparing results obtained under two different chain models, one can delineate the effect of excluded volume interaction on the partitioning of polymer chains into the pore.

In the current study, we investigate the partitioning of star polymers into pores under SEC, LCCC and LAC conditions. The motivation of such theoretical study stems from the need to characterize branched polymers. Branched polymers are encountered frequently in synthetic polymers like polyolefins or in natural polymers like polysaccharides. Branching can significantly affect properties of polymers and therefore characterization of branching structures is an important step. SEC can be used to obtain the hydrodynamic volume of branched polymers [18,19] since the universal calibration is still valid. However, when SEC is used to characterize statistically branched polymers, each slice in SEC elution contains a range of molecular weights [20], and this considerably lower the accuracy of the determination of molecular weight distributions. Hence, investigators recently have attempted to characterize branched polymers with interactive chromatography [21–32]. One of the questions that arise from these recent experimental investigations is whether star polymers should elute together at the LCCC condition with their counterpart of linear polymers. Finding the answer to this question in experiments is plagued by the fact that in most cases stars prepared in experiments will chemically differ from their counterpart linear polymers. Theory based on Gaussian chain has predicted that stars should elute together with linear polymers if their chemical structures are exactly the same. This prediction however ignores one important factor, the excluded volume interaction in polymers. Here we make use of computer simulations and examine the partitioning of star branched polymers with two different chain models, random walks (RW) and self-avoiding walks (SAW). We present computer simulation results for the two models and discuss the effect of excluded volume on the elution of star polymers in three different chromatography modes.

## 2. Simulation methods

All simulations reported here were performed on simple cubic lattice with coordination number  $z=26$ . A schematic drawing illustrates the 26 neighboring sites is shown in Fig. 1. In the random walks (RW) model, beads on polymer chains may occupy the same site on the lattice. In the self-avoiding walk (SAW) model, no two beads are allowed to occupy the same site, but bonds may cross each

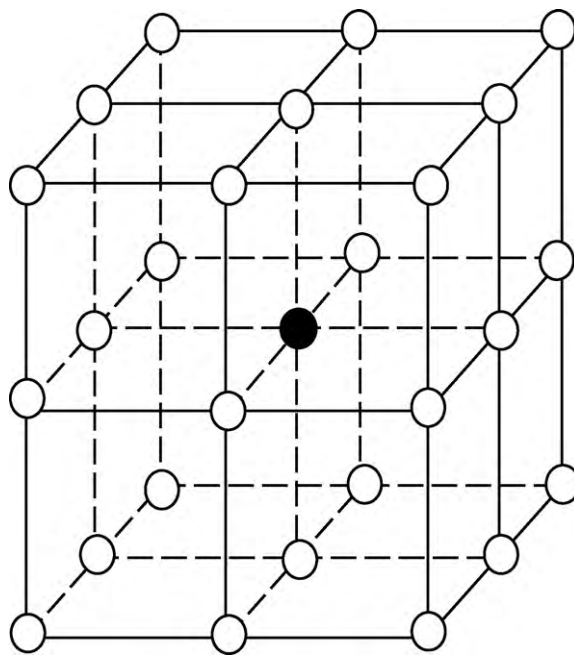


Fig. 1. A schematic drawing showing the 26 neighboring sites (white circles) around the central site (the dark circle).

other. This unrealistic crossing in SAW model however should not affect the static conformational properties.

We investigated the partitioning of star branched polymers into slit pores. The slit pore is modeled as a cubic lattice with dimensions of  $100a \times 100a \times (D+1)a$  along  $X$ ,  $Y$  and  $Z$  directions respectively, where  $a$  is the lattice unit length. Periodic boundary conditions are applied in the  $X$  and  $Y$  directions. There are two solid impenetrable walls located at  $Z=a$ , and  $Z=(D+1)a$ . Typical values of  $D$  used are 14–29. The star polymers are modeled by  $f$  arms consisting of  $N_a$  monomers (or beads) connected to a central bead. The total number of beads in a star is given by  $N_{\text{tot}} = fN_a + 1$ . We have studied series of stars with  $f=2, 3, 4, 5, 6, 7, 8$  and total beads  $N_{\text{tot}}$  ranged from 48 to 312. Data are presented for each set of stars with a given  $f$ , varying arm length such that  $N_{\text{tot}}$  may cover the range from 48 to 312. A surface interaction,  $\varepsilon_w$ , reduced by the Boltzmann factor,  $\beta = 1/k_B T = 1$ , is applied to any beads located next to the wall and is applied between the bead and all neighboring surface sites equally. In  $z=26$  model, the number of surface sites a monomer may interact with is  $n_{\text{surf}}=9$  (see the nine sites below the central site shown in Fig. 1). No other interactions are applied in this study. The standard chemical potential of the stars inside the slit, reduced by the Boltzmann factor,  $\mu_{\text{in}}^0$ , is determined by biased chain insertion. Details of the method can be found in Refs. [7,9,33–36]. The partition coefficient of the stars in the slit  $K$  is given by  $\ln K = -(\mu_{\text{in}}^0 - \mu_{\text{bulk}}^0)$ ,  $\mu_{\text{bulk}}^0$  is the standard chemical potential of the chain in the bulk solution, modeled by a cubic lattice of dimension  $100a \times 100a \times 100a$  with periodic boundary conditions applied in all three directions. In addition to the determination of the partition coefficient, the radius of gyration of the stars along the  $X$ ,  $Y$  and  $Z$  directions are determined as well. These quantities are labeled as  $R_{g,XY}$  and  $R_{g,Z}$  respectively and they are calculated based on the following equations:

$$R_{g,XY}^2 = \frac{1}{N} \left\langle \sum_{i=1}^N [(X_i - X_{\text{cm}})^2 + (Y_i - Y_{\text{cm}})^2] \right\rangle;$$

$$R_{g,Z}^2 = \frac{1}{N} \left\langle \sum_{i=1}^N [(Z_i - Z_{\text{cm}})^2] \right\rangle \quad (1)$$

where  $X_{cm}$ ,  $Y_{cm}$ , and  $Z_{cm}$  are the center of mass of the chain in three directions, the brackets stand for ensemble average over all possible conformations. In addition, the radius of gyration of the stars in the bulk solution have also been determined and are labeled as  $R_{g0}$ , without differentiating the X, Y and Z directions since the chains adopt isotropic orientations in the bulk solution. We have also calculated the hydrodynamic radius,  $R_H$ , for the chains in bulk solution according to the following definition [37]:

$$\frac{1}{R_H} = \frac{1}{N^2} \left\langle \frac{1}{\sum_{m \neq n, m, n=1}^N [(X_m - X_n)^2 + (Y_m - Y_n)^2 + (Z_m - Z_n)^2]^{1/2}} \right\rangle \quad (2)$$

This hydrodynamic radius follows from Kirkwood approximation to treat hydrodynamic interaction for polymers in dilute solution [38]. Numerical determination of the hydrodynamic radius is performed based on generated static conformations, which can be easily done for chains modeled by SAW, but unfortunately can not be determined for random walks since some of beads may overlap with each other, which yield undefined values in Eq. (2).

### 3. Results and discussion

#### 3.1. Partitioning of stars into pores when modeled as random walks

We first present simulation results obtained when star branched polymers are modeled as random walks (RW stars). These results will serve as the basis for further discussion on results obtained for stars modeled by SAW (SAW stars) where excluded volume interaction is present.

The static conformation of star polymers has been discussed by Zimm and Stockmayer [38]. They have defined a branching parameter to quantify the difference of star polymers from that of linear polymers with the same total molecular weight. The branching parameter  $g$  is defined as the ratio of mean square radius of gyration of stars and linear chains with equal number of segments:

$$g(f) = \frac{\langle R_g^2 \rangle_f}{\langle R_g^2 \rangle_{f=2}} \quad (3)$$

where  $f$  is the number of arms in the star. Using the Gaussian chain model, Zimm and Stockmayer showed that  $g(f) = (3f - 2)/f^2$  when the chain length  $N \gg 1$  [37]. Fig. 2 confirms that Eq. (1) holds. All five curves fall neatly on the master trend line when  $R_{g0}^2$  determined for the star is reduced by the  $g$  factor. It is important to note that the relationship illustrated in Fig. 2 refers to values obtained for stars in bulk solution. When stars are placed in the slit, such relationship will no longer hold.

The RW model has a number of deficiencies in modeling real polymers. One such deficiency is that when polymers modeled by RW are placed in pores, the dimension of the polymers parallel to the pore walls is not affected by the confinement. This is an artifact due to the random walks model [17]. Fig. 3 illustrates this deficiency where  $R_{g,XY}$  and  $R_{g,Z}$  for stars placed inside the slit, each reduced by their corresponding values in the dilute bulk solution, are presented against  $D/R_{g0}$  where  $D$  is the slit width.  $R_{g,Z}$  is the radius of gyration component in the Z direction where the walls exists. Monomers of the star polymers are not allowed to exist on or beyond the slit walls. Therefore, when a slit width shrinks in the Z direction,  $R_{g,Z}$  of the polymers likewise decreases. This decrease is only significant when  $D$  and  $R_{g0}$  of polymers become comparable in size. From Fig. 3, one can observe that when  $D/R_{g0} < 4.0$ , the Z-component decreases due to the confinement. However, the XY-component is not affected at all. We will shortly show that this is not the case for the SAW model. In addition, one can notice that data for the Z-component

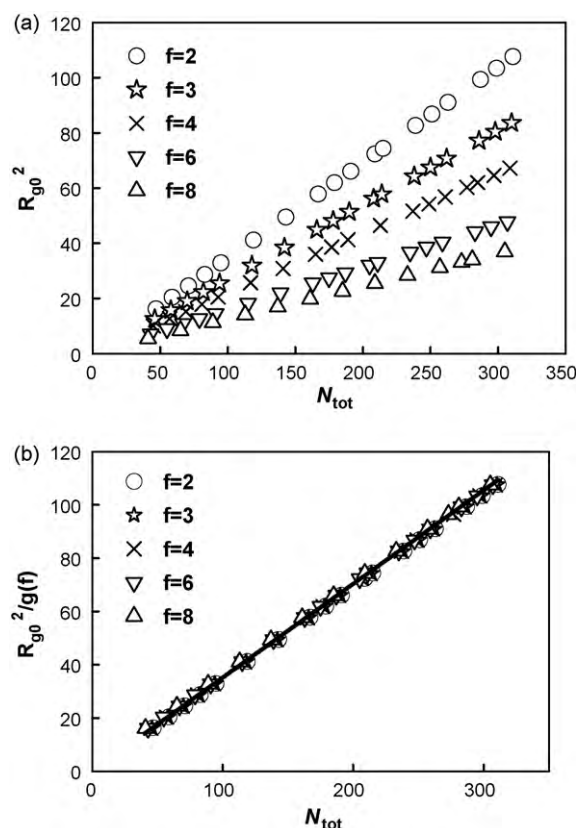
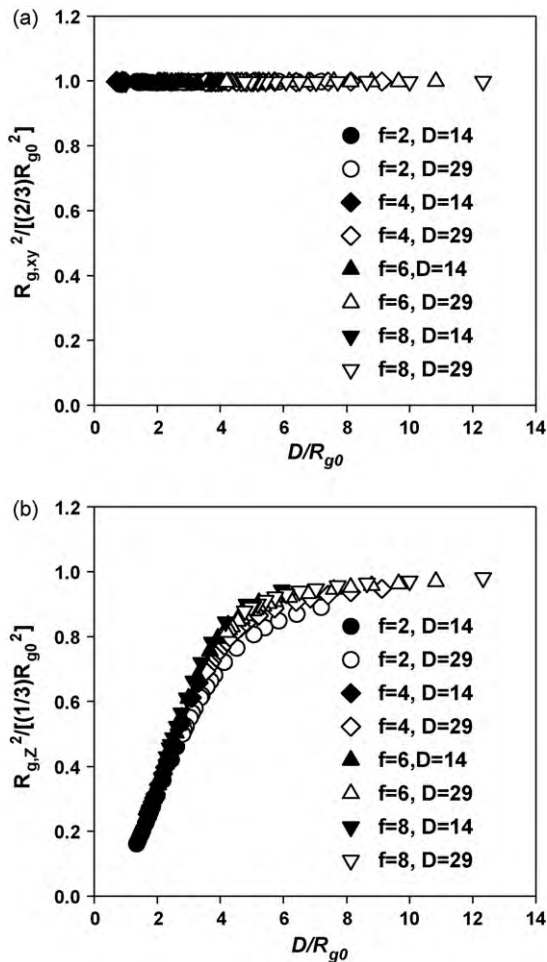


Fig. 2. Plot of radius gyration of RW star polymers in bulk solution: (a)  $R_{g0}^2$  vs.  $N_{tot}$  and (b)  $R_{g0}^2/g(f)$  vs.  $N_{tot}$  for  $f=2, 3, 4, 6,$  and  $8$ ;  $g(f) = ((3f - 2)/f^2)$ . The solid line in (b) is the power-law fit with exponent of 1.0.

with different arm numbers do not form a master curve. Data sets with high  $f$  lie slightly above data sets for smaller  $f$ . This implies that if branched polymers and linear polymers have the same  $R_g$  in the bulk solution, when placed in the pore, the linear polymers will contract more in the Z direction than the branched structures. We will see shortly that this phenomenon is still retained when stars are modeled by SAW.

The most important variable when studying the partitioning of polymers – or any species for that matter – is the partition coefficient,  $K$ . Here, a higher partition coefficient indicates a lower chemical potential of polymers when placed inside the slit and therefore more extensive entry of polymers into the slit. The partitioning of star polymers into pores in SEC condition (i.e., no surface interaction,  $\varepsilon_w = 0$ ) has been studied earlier by Casassa [12,13] and recently discussed again by Teraoka [39]. Unlike linear polymers, the partition coefficient  $K$  for star polymers do not form a common curve when plotted against  $R_{g0}/D$ . Fig. 4 presents the plot of  $K$  vs.  $R_{g0}/D$  for star branched polymers with different number of arms,  $f=2, 4$  and  $8$  in two slit widths,  $D=14$  and  $29$ . Data for fixed arm numbers but different slit width nearly form a common curve although some deviation is seen for  $f=8$  data. But data sets for different arm numbers do not overlap with each other. Teraoka suggested that a plot of  $K$  vs.  $R_H/D$  for star branched polymers would yield a common curve. Unfortunately for random walks, we cannot determine  $R_H$  numerically in the simulations.

The critical condition in LCCC is the critical adsorption point (CAP) of linear polymers above the solid surface. For chains modeled as RW in our simulation, the CAP can be calculated using the condition:  $n_{surf} \varepsilon_w^{CC} = -\ln(z/(z - B))$ , where  $z$  is coordination number in the chain model, and  $B$  is the number of directions forbidden due to presence of the walls (see p. 112 in Ref. [40]). In



**Fig. 3.** Plot of radius of gyration of RW stars in a slit pore reduced by their corresponding values in bulk solution. (a) Parallel component,  $R_{g,xy}^2/[(2/3)R_{g0}^2]$  vs.  $D/R_{g0}$ ; (b) perpendicular component,  $R_{g,z}^2/[(1/3)R_{g0}^2]$  vs.  $D/R_{g0}$ . No surface interaction ( $\epsilon_w = 0$ ).

our simulation model,  $B=9$  in a slit pore and  $z=26$ . This leads to  $\epsilon_w(\text{CAP}) = -0.047$ . This CAP was confirmed numerically by using the approach proposed by our group [9,36,41], namely, a plot of standard deviation in  $\ln K$  for a given set of chain lengths of linear chains vs.  $\epsilon_w$  that will give the minimum in such plot which is the CAP point. Fig. 5 presents the plot of  $K$  at the CAP vs. total beads  $N_{\text{tot}}$

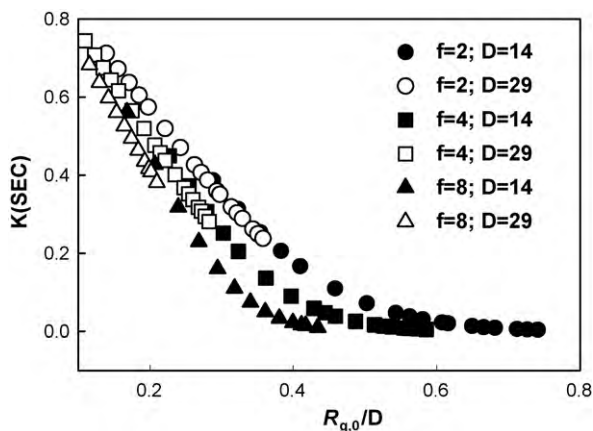


**Fig. 4.** Partition coefficient  $K$  for RW stars in SEC (i.e.,  $\epsilon_w = 0$ ) vs.  $R_{g0}/D$  for stars with arm number  $f=2, 4,$  and  $8$  in slit pore of width  $D=14$  and  $29$ .

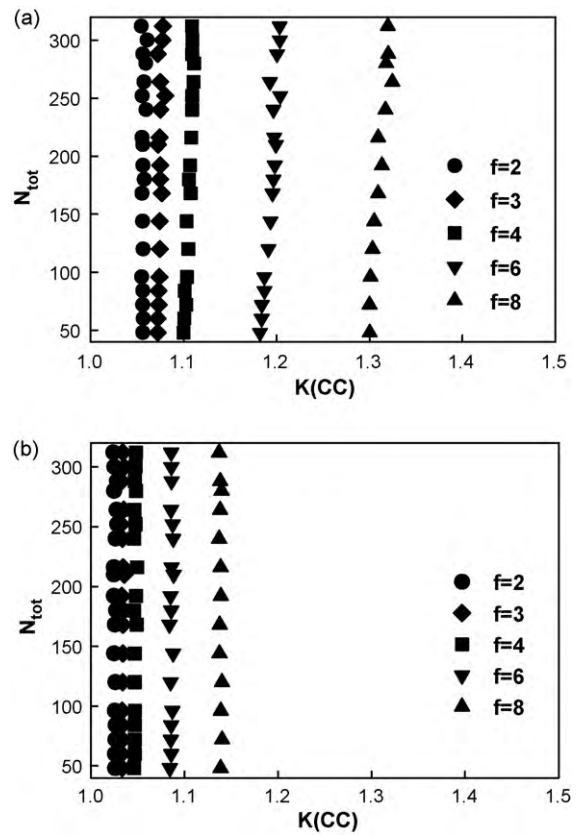


**Fig. 5.** Plot of  $N_{\text{tot}}$  vs.  $K$  in LCCC condition (i.e.,  $\epsilon_w = \epsilon_w(\text{CAP}) = -0.047$ ) for RW stars with  $f=2, 3, 4,$  and  $8$  in (a)  $D=14$  and (b)  $D=29$  slit.

for sets of stars with different arm numbers and arm lengths. A few patterns are immediately apparent in Fig. 5. Firstly, we notice that at the CAP,  $K$  for stars with different arm length but same number of arms ( $f$  fixed) form vertical straight lines. The  $f=2$  data set (i.e., the linear polymers) confirms that the CAP is the critical condition (CC) since a straight vertical line indicates co-elution for linear polymers, a condition typically employed in experiments to identify the critical condition. Secondly,  $K(\text{CC})$  for stars with different arm numbers are not exactly the same. The larger  $f$ , the larger the  $K(\text{CC})$ . Also, the smaller the slit width, the larger the difference in  $K(\text{CC})$  with different  $f$ . This may appear as surprising to the common understanding of  $K$  in the critical condition. The usual notion is that  $K=1$  and is independent of slit width, chain length and star architecture

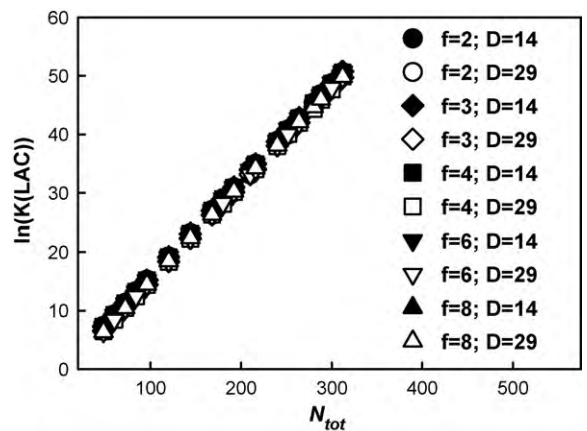


**Fig. 6.** Plots of  $K$  in LAC mode as a function of total number of beads in RW star polymers when  $\epsilon_w = -0.10$ .

at the critical condition. This notion comes from the theoretical calculation based on the Gaussian chain model. Here the chains are modeled as RW. The usual understanding is that results from RW will reproduce theoretical calculations based on Gaussian chain model. Actually, lattice based RW model is not completely equivalent to the continuum based Gaussian chain model as discussed by Guttman et al. [6]. The treatment of the CAP point in the Gaussian chain model missed small subtle effect. The CAP is defined in the infinite long chain limit. At the CAP, the entropic exclusion is perfectly compensated by enthalpic adsorption for the middle beads, but not for the two end beads. The free energy change of the end beads at the CAP is slightly negative, leads to a  $K$  being greater than one. The more arms the star has, the more end beads it has, the larger the  $K$  value. Same results were reported by Guttman et al. [6] in their Fig. 6. If the length of arms were infinitely long, then the partition coefficients  $K$  will all approach one as shown by Guttman et al. The continuum theory using Gaussian chain model missed this effect because of the use of continuous flight chain model. We want to point out however that the difference in  $K$  shown in Fig. 5 is small and it gets smaller if the pore size is large. Shortly we will present results for stars modeled as SAW in LCCC. The mechanism that leads to slightly more adsorptive ends is still under play, but excluded volume interaction adds another layer of complexity in the obtained partition coefficient. The partition coefficients differ much more significantly than those observed here for RW. Also here  $K(\text{CC})$  depends on  $f$  and  $D$  only, not on the arm length since data sets for given  $f$  mostly form a vertical straight line. As will be seen later, this pattern will not hold at the critical adsorption point when excluded volume interactions are introduced.

When surface attraction  $\varepsilon_w$  increases beyond CAP point  $\varepsilon_w(\text{CAP})$ , one enters the LAC mode of elution. For random walks, the partitioning coefficient of polymers in LAC is generally believed [24] to depend only on the total number of beads, and not be sensitive to the chain architecture. This was indeed found to be true. Fig. 6 presents  $K$  determined for the stars when  $\varepsilon_w = -0.10$ . A linear dependence of  $\ln K(\text{LAC})$  on  $N_{\text{tot}}$  is observed and stars with different  $f$  and  $D$  form a common curve.

### 3.2. Partitioning of stars into pores when modeled as self-avoiding walks

Now we present corresponding results for SAW stars. Fig. 7 presents the dependence of radius of gyration of stars in the bulk solution,  $R_{g0}^2$ , as a function of  $N_{\text{tot}}$ . For the SAW model, the same branching parameter  $g(f)$  proposed by Zimm and Stockmayer can be used to rescale the dependence of  $R_{g0}^2$  on  $N_{\text{tot}}$  for stars with different number of arms as shown in Fig. 7(b). There are deviations from the master plot in Fig. 7(b) that were not observed in Fig. 2(b). Stars with low  $f$  values have slightly higher  $R_{g0}^2/g(f)$  values at a given  $N_{\text{tot}}$  than stars with higher  $f$ . The deviation however is very small. Several earlier studies have found this  $g(f)$  to be applicable [42], including our recent simulations with dissipative particle dynamics [43]. We note that  $R_{g0}^2/g(f)$  is found to scale with  $N_{\text{tot}}$  with an exponent 1.2,  $R_{g0}^2/g(f) \sim N_{\text{tot}}^{1.2}$ , an exponent value expected for chains with excluded volume interaction.

Fig. 8 presents the  $R_{g,XY}$  and  $R_{g,Z}$  for SAW stars placed inside the slit when  $\varepsilon_w = 0$ . Unlike in the RW, now the parallel component increases as the chains are confined in the slit, a more realistic representation of what will actually happen to a real polymer chain being confined in the pore.

Fig. 9 presents plot of  $K$  in SEC for SAW stars, where  $K(\text{SEC})$  is plotted against  $R_{g0}/D$  in (a) and as  $R_H/D$  in (b). A much better scaling plot is obtained when  $K(\text{SEC})$  is plotted against  $R_H/D$ , as suggested by Teraoka [39], but nevertheless the scaling is not perfect even in the latter case.

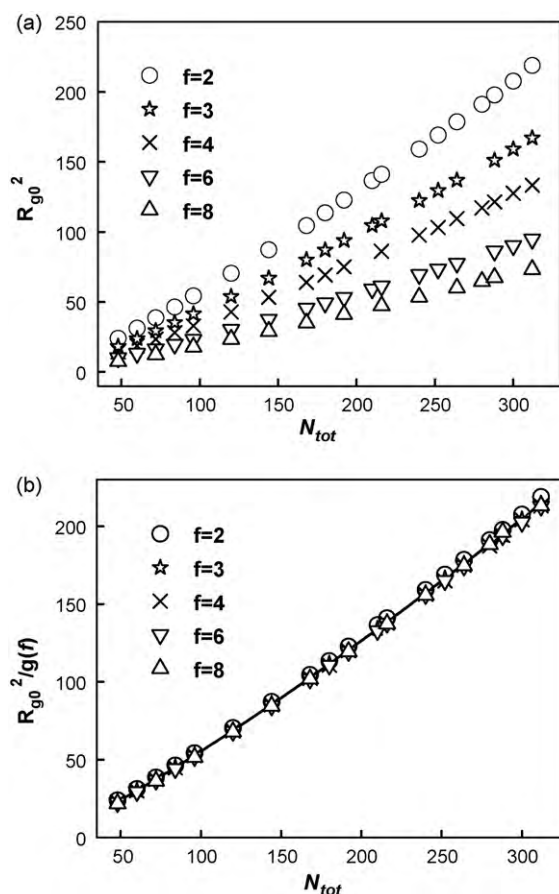
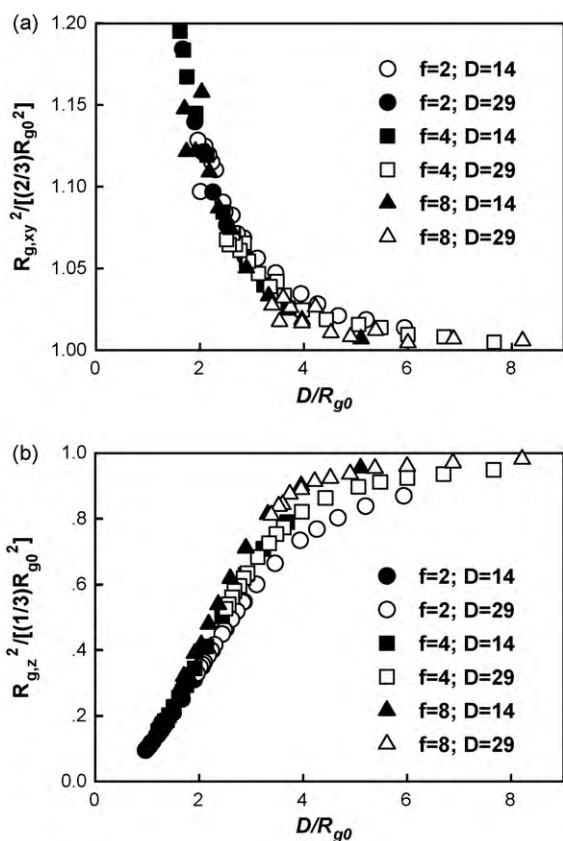


Fig. 7. Plot of radius gyration of SAW star polymers in bulk solution: (a)  $R_{g0}^2$  vs.  $N_{\text{tot}}$ ; (b)  $R_{g0}^2/g(f)$  vs.  $N_{\text{tot}}$  for  $f=2, 3, 4, 6$ , and  $8$ ;  $g(f) = ((3f-2)/f)^2$ . Solid line in (b) is the power-law fit with an exponent of 1.19.

The CAP for SAW model cannot be calculated theoretically, but needs to be determined numerically in the simulations. We identified CAP to be at  $\varepsilon_w = -0.061$  using linear chains (results will be shown in Fig. 11). This CAP value is larger than that in RW model, which is to be expected since one might envision that it takes more enthalpic attraction to compensate the entropic exclusion for a chain with excluded volume interaction. Fig. 10 presents the  $K(\text{CC})$  for stars at the CAP in two different slit widths for SAW stars. Comparing the plots in Figs. 10 and 5 reveals the following difference. Data sets for a given  $f$  in Fig. 10 do not form vertical straight lines like that in Fig. 5. This curvature effect has been repeatedly observed when chains are modeled by SAW [9,36,41,44]. The error bars associated with calculated  $K(\text{CC})$  for SAW stars are large as can be seen in the scattered data points for each set of data. Secondly, stars with high number of  $f$  at the same  $N_{\text{tot}}$  tend to have smaller  $K$  when  $N_{\text{tot}}$  is large, but a reversed behavior is seen when  $N_{\text{tot}}$  is low (i.e., very short arms). There are two effects under play here. The end beads of SAW stars are slightly adsorptive in the pore just as in the case of RW stars. Stars with short arms but high  $f$  have  $K$  values larger than that of linear chains (see data point for  $f=8$  when  $N_{\text{tot}}=50$ ). This first effect however is weak. The second more pronounced effect is the excluded volume interaction. The densities of stars around the cores increase as  $f$  increases when  $N_{\text{tot}}$  is kept fixed. A denser core thus experiences greater excluded volume interaction which leads to more entropic repulsion especially when pore size is small. In  $D=14$ ,  $K(\text{CC})$  for stars with  $f=6$  and  $8$  become less than 1.0 when  $N_{\text{tot}}$  is high. Notice, on the other hand, that even though there is deviation from a vertical straight line, all values of  $K(\text{CC})$  for  $f=2$  (linear chains) remain greater than 1.0. These results suggest that



**Fig. 8.** Plot of radius of gyration of SAW stars in a slit pore reduced by their corresponding values in bulk solution. (a) Parallel component,  $R_{g,xy}^2 / [(2/3)R_{g0}^2]$  vs.  $D/R_{g0}$ ; (b) Perpendicular component,  $R_{g,z}^2 / [(1/3)R_{g0}^2]$  vs.  $D/R_{g0}$ . No surface interaction ( $\varepsilon_w = 0$ ).

stars with high number of arms can be in exclusion mode when chromatography condition remains in LCCC mode for the correspondingly linear chains. This phenomenon has been observed in experiments by Chang's group [30]. Seeing the strong dependence of  $K$  on  $N_{tot}$  for stars, one might wonder if the critical condition in LCCC might be shifted for stars. Fig. 11 presents the plots of standard deviation in  $\ln K$  vs.  $\varepsilon_w$  for stars with given  $f$  but varying arm length. We see that minima are still located at  $\varepsilon_w = -0.061$  for all the stars. Hence this is still the "Critical Condition" point.

Fig. 12, comparable to Fig. 6, presents the plot of  $\ln K$  vs.  $N_{tot}$  in LAC mode when  $\varepsilon_w = -0.1 < \varepsilon_w(\text{CAP})$ . Unlike in Fig. 6, now we see that data sets for different  $f$  and  $D$  do not form a collapsed line. While the total number of beads is still a dominant factor that determines the  $K(\text{LAC})$  for the stars,  $K(\text{LAC})$  however also depends on  $f$  and  $D$ . In general,  $K(\text{LAC})$  decreases with an increase in  $f$  and  $D$ . The higher the number of arms, the smaller the  $K$ , since stars with high number of  $f$  will experience greater repulsion in the slit, hence reducing the  $K$ . The effect of  $D$  on  $K$  is due to adsorption of stars on both surfaces. When  $D$  is small, the two adsorbing surfaces are close and may act cooperatively to increase the  $K$ .

Recently Radke et al. examined the retention behavior of linear, branched and hyperbranched polyesters in interactive liquid chromatography [45]. In gradient LAC, the degree of branching was found to affect the retention volume. However, the retention volume increased with the degree of branching, opposite to the trend displayed in Fig. 12. Although one may argue that the branched polymers studied in Radke's paper is not star branched polymer, hence one may expect a different behavior from that of star branched polymers. However, we suspect that the dependence of elution volume on the branching retains the same for these

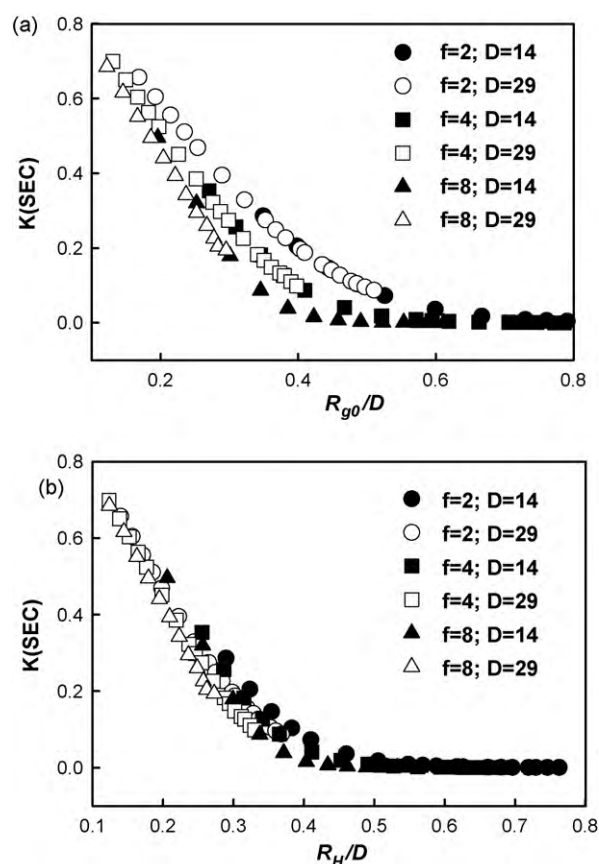


**Fig. 9.** Partition coefficient  $K$  in SEC (i.e.,  $\varepsilon_w = 0$ ) vs.  $R_{g0}/D$  for SAW stars with arm number  $f = 2, 4, \text{ and } 8$  in slit pore of width  $D = 14$  and  $29$ . (a)  $K(\text{SEC})$  vs.  $R_{g0}/D$ ; (b)  $K(\text{SEC})$  vs.  $R_H/D$ .

branched polymers if surface interactions of the repeating units in branched structures are the same. In another words, at the same given total molecular weight, increase in the degree of branching will lead to smaller retention time if there is no difference in the chemical structures. The possible explanation to the results in Radke's paper is that as the degree of branching increases, the percent of repeating units that are more adsorptive also increases. The observed increase in elution time with the degree of branching is not due to topological effect, but due to chemical difference in the branching point. This is another example illustrating the complexity in the elution mechanism of branched polymers in interactive chromatography.

#### 4. Conclusion

Excluded volume interaction between polymer segments along the chain is long known to be an important factor in determining physical properties of polymer systems. Often this interaction can lead to different behavior when compared with theoretical predictions that ignored such interactions. Here we investigate how the excluded volume interaction, which is ignored in most theoretical calculations of polymer partitioning, will affect the partitioning of polymers. In particular, we focus on the star branched polymers since the excluded volume interaction for stars in the pores can be very significant. We present Monte Carlo simulation results on the partitioning of star branched polymers into slit pores at three chromatography conditions, SEC ( $\varepsilon_w = 0$ ), LCCC ( $\varepsilon_w = \varepsilon_w(\text{CAP})$ ), and LAC ( $|\varepsilon_w| > \varepsilon_w(\text{CAP})$ ). Simulations have been performed for two chain models, random walks (RW) and self-avoiding walk (SAW). Comparison of the results between two chain models reveals the effect

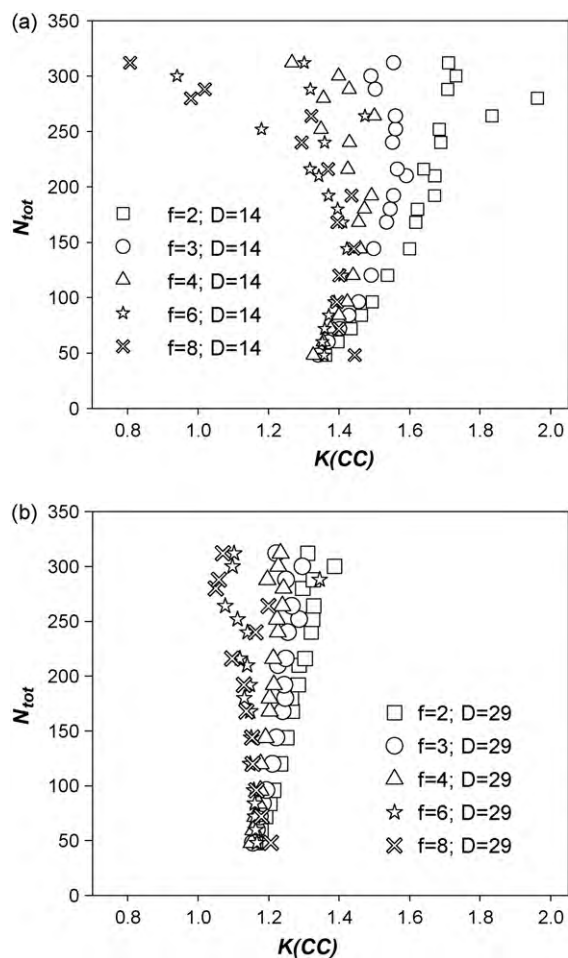


**Fig. 10.** Plot of  $N_{\text{tot}}$  vs.  $K$  in LCCC condition (i.e.,  $\varepsilon_w = \varepsilon_w(\text{CAP}) = -0.061$ ) for SAW stars with  $f=2, 3, 4, 6,$  and  $8$  in (a)  $D=14$ , and (b)  $D=29$ .

of excluded volume interaction on the partitioning rules. The two outstanding differences revealed by the SAW model are: (1) in LCCC, stars with high number of arms can be excluded from small pores; (2) in LAC mode,  $K(\text{LAC})$  is not entirely determined by the total number of beads in stars. Highly branched polymers with the same  $N_{\text{tot}}$  but high  $f$  will have smaller  $K$  in LAC mode.

We would like to finally emphasize that the excluded volume interaction is not just an effect that needs to be considered only if the solvent is a good solvent. Although it is often stated that

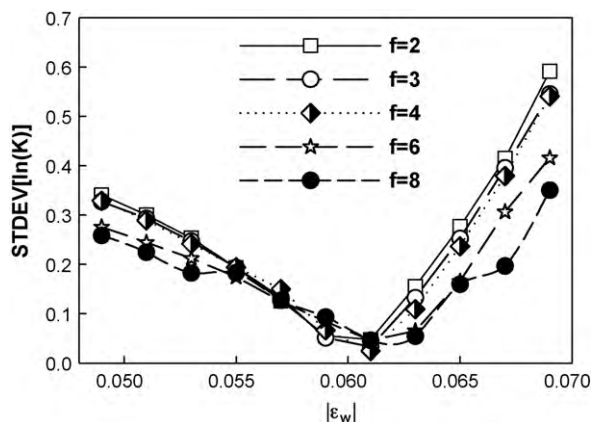


**Fig. 11.** Plot of deviation in  $\ln K$  vs.  $|\varepsilon_w|$  for SAW stars with  $f=2, 3, 4, 6,$  and  $8$  in slit pore of width  $D=30a$ . The  $\varepsilon_w(\text{CAP}) = -0.061$  is identified as the minima on the plots.

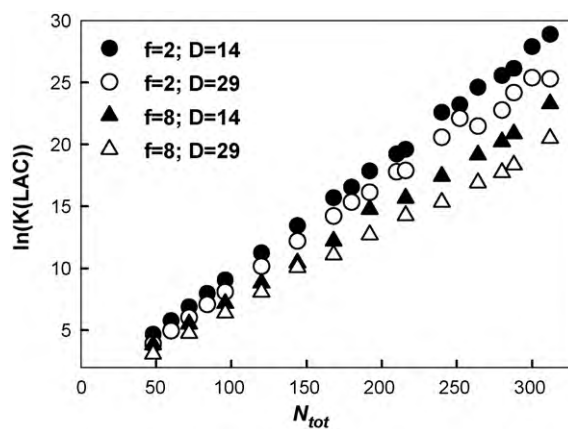


**Fig. 12.** Plot of  $\ln K$  vs.  $N_{\text{tot}}$  for SAW stars with  $f=2,$  and  $8; D=14$  and  $29$  in LAC mode;  $\varepsilon_w = -0.1$  which is much lower than the CAP.

the Gaussian chain model is applicable if solvent is in theta solvent. This statement nevertheless is only valid when discussing some aspects of physical properties of polymers. A real polymer chain never behaves like a Gaussian chain, even in theta solvent. In theta solvent, the effect of excluded volume interaction is reduced because of attraction between monomers in theta solvents such that the second virial coefficient becomes zero. The statistics of the chain in theta solvent follows closely to that of the Gaussian chain model. However, the monomer overlap is still strictly forbidden even for a real polymer chain in theta solvent [41]. The use of the Gaussian chain model to treat polymers confined in pores is exasperated by the problem of excluded volume interaction as the chance of monomer overlaps become increasingly high when confined in the pore. Hence, when interpreting chromatography separations of polymers in various modes, it is important to keep in mind of the effect of excluded volume interactions on the partitioning rules as presented in this report.

## Acknowledgements

This research is supported by partial financial funding from ACS/PRF (PRF# 46933-AC7) and from National Science Foundation under Grant Number CHE-0724117 (co-funded by MPS/CHE and OISE).

## References

- [1] Z. Grubisic, P. Rempp, H. Benoit, *J. Polym. Sci. Part B: Polym. Lett.* 5 (1967) 753.
- [2] H. Pasch, B. Trathnigg, *HPLC of Polymers*, Springer-Verlag, Berlin/Heidelberg, 1999.
- [3] T. Chang, *Adv. Polym. Sci.* 163 (2003) 1.
- [4] M.K. Kosmas, E.P. Bokaris, E.G. Georgaka, *Polymer* 39 (1998) 4973.
- [5] A.M. Skvortsov, A.A. Gorbunov, D. Berek, B. Trathnigg, *Polymer* 39 (1998) 423.
- [6] C.M. Guttman, E.A. DiMarzio, J.F. Douglas, *Macromolecules* 29 (1996) 5723.
- [7] Y. Gong, Y. Wang, *Macromolecules* 35 (2002) 7492.
- [8] A. Gorbunov, B. Trathnigg, *J. Chromatogr. A* 955 (2002) 9.
- [9] S. Orelli, W. Jiang, Y. Wang, *Macromolecules* 37 (2004) 10073.
- [10] D. Berek, *Macromolecules* 31 (1998) 8517.
- [11] D. Berek, *Macromol. Symp.* 258 (2007) 198.
- [12] E.F. Casassa, *J. Polym. Sci. Part B: Polym. Lett.* 5 (1967) 773.
- [13] E.F. Casassa, Y. Tagami, *Macromolecules* 2 (1969) 14.
- [14] A.A. Gorbunov, A.V. Vakhrushev, *J. Chromatogr. A* 1064 (2005) 169.
- [15] A.A. Gorbunov, A.V. Vakhrushev, *Polymer* 50 (2009) 2727.
- [16] W. Lee, H. Lee, H.C. Lee, D. Cho, T. Chang, A.A. Gorbunov, J. Roovers, *Macromolecules* 35 (2002) 529.
- [17] P.G. De Gennes, *Scaling Concepts in Polymer Physics*, Cornell University Press, Ithaca, 1979.
- [18] A.E. Hamielec, A.C. Ouano, *J. Liq. Chromatogr.* 1 (1978) 111.
- [19] A.E. Hamielec, A.C. Ouano, L.L. Nebenzahl, *J. Liq. Chromatogr.* 1 (1978) 527.
- [20] M. Gaborieau, J. Nicolas, M. Save, B. Charleux, J.P. Vairon, R.G. Gilbert, P. Castignolles, *J. Chromatogr. A* 1190 (2008) 215.
- [21] I. Park, S. Park, D. Cho, T. Chang, E. Kim, K. Lee, Y.J. Kim, *Macromolecules* 36 (2003) 8539.

- [22] K. Min, H. Gao, K. Matyjaszewski, *J. Am. Chem. Soc.* 127 (2005) 3825.
- [23] W. Radke, K. Rode, A.V. Gorshkov, T. Biela, *Polymer* 46 (2005) 5456.
- [24] J. Gerber, W. Radke, *Polymer* 46 (2005) 9224.
- [25] D.M. Meunier, P.B. Smith, S.A. Baker, *Macromolecules* 38 (2005) 5313.
- [26] M. Li, N.M. Jahed, K.e. Min, K. Matyjaszewski, *Macromolecules* 37 (2004) 2434.
- [27] H. Gao, K.E. Min, K. Matyjaszewski, *Macromol. Chem. Phys.* 207 (2006) 1709.
- [28] T. Macko, H. Pasch, *Macromolecules* 42 (2009) 6063.
- [29] A.V. Vakhrushev, A.A. Gorbunov, Y. Tezuka, A. Tsuchitani, H. Oike, *Anal. Chem.* 80 (2008) 8153.
- [30] K. Im, H.W. Park, Y. Kim, S. Ahn, T. Chang, K. Lee, H.J. Lee, J. Ziebarth, Y. Wang, *Macromolecules* 41 (2008) 3375.
- [31] R. Edam, D.M. Meunier, E.P.C. Mes, F.A. Van Damme, P.J. Schoenmakers, *J. Chromatogr. A* 1201 (2008) 208.
- [32] H. Gao, K. Matyjaszewski, *J. Am. Chem. Soc.* 129 (2007) 11828.
- [33] Y. Wang, I. Teraoka, *Macromolecules* 33 (2000) 3478.
- [34] Y. Wang, *J. Chem. Phys.* 121 (2004) 3898.
- [35] D. Frenkel, B. Smit, *Understanding Molecular Simulations—From Algorithms to Applications*, Academic Press, San Diego, CA, 2002.
- [36] J.D. Ziebarth, Y. Wang, A. Polotsky, M. Luo, *Macromolecules* 40 (2007) 3498.
- [37] I. Teraoka, *Polymer Solutions: An Introduction to Physical Properties*, Wiley-Interscience, 2002.
- [38] B.H. Zimm, W.H. Stockmayer, *J. Chem. Phys.* 17 (1949) 1301.
- [39] I. Teraoka, *Macromolecules* 37 (2004) 6632.
- [40] G.J. Fleer, M.A. Cohen Stuart, J.M.H.M. Scheutjens, T. Cosgrove, B. Vincent, *Polymers at Interfaces*, Chapman & Hall, London, UK, 1993.
- [41] J. Ziebarth, S. Orelli, Y. Wang, *Polymer* 46 (2005) 10450.
- [42] K. Shida, K. Ohno, M. Kimura, Y. Kawazoe, Y. Nakamura, *Macromolecules* 31 (1998) 2343.
- [43] Z. Li, Y. Li, Y. Wang, Z. Sun, L. An, *Macromolecules* 43 (2010) 5896.
- [44] Y. Zhu, J. Ziebarth, T. Macko, Y. Wang, *Macromolecules* 43 (2010) 5888.
- [45] M. Al Samman, W. Radke, A. Khalyavina, A. Lederer, *Macromolecules* 43 (2010) 3215.